

Inclusive and Exclusive $|V_{ub}|$

A. Petrella on behalf of *BABAR* and Belle Collaborations
Università degli Studi and INFN, Ferrara, Italy

The current status of the determinations of CKM matrix element $|V_{ub}|$ via exclusive and inclusive charmless semileptonic B decays is reviewed.

1. Introduction

In the Standard Model (SM), weak transitions between quark flavours are described by the elements V_{ij} of the Cabibbo Kobayashi Maskawa (CKM)[1] matrix. Theory does not predict the magnitude of the elements which therefore must be determined experimentally. The matrix is unitary by construction and one of the unitarity conditions, $V_{ud}V_{ub}^* + V_{cd}V_{cb}^* + V_{td}V_{tb}^* = 0$, can be geometrically represented as a triangle in the complex plane $(\bar{\rho}, \bar{\eta})^1$, the well known Unitarity Triangle (UT). Any non zero value of the $\bar{\eta}$ parameter is an indication of CP violation. The angles and sides of the UT can be measured studying B meson decays.

The Unitarity Triangle analysis shows an impressive success of the CKM picture in describing CP violation in the SM, but, as the experimental results become increasingly precise, a slight disagreement between the angle β , characterising indirect CP violation in $b \rightarrow \bar{c}cs$ transitions, currently known at the 4% level, and $|V_{ub}|/|V_{cb}|$ has appeared in the UT fit. This disagreement could be due to some problems with theoretical calculation on $|V_{ub}|$ determinations. Tree-level processes are essentially immune to contribution from new physics, so studying semileptonic B decays and therefore determining $|V_{cb}|$ and $|V_{ub}|$, is a way to test the electroweak sector of the SM. While the determination of $|V_{cb}|$ is at the 2% level [2], the uncertainty on $|V_{ub}|$ is still at the 8% level. The need for an improvement in the precision on $|V_{ub}|$ is therefore evident.

In the following we will present the current status and outlook of experimental determinations of $|V_{ub}|$.

2. Semileptonic B Decays

The theoretical description of charmless semileptonic B decays is at mature stage. $\bar{B} \rightarrow X_u \ell \bar{\nu}$ decays provide the cleanest way to measure $|V_{ub}|$ since the leptonic and hadronic part of the weak current factorize into two terms not interacting between each other,

¹ $\bar{\rho} = (1 - \lambda^2/2)\rho$, $\bar{\eta} = (1 - \lambda^2/2)\eta$, where $\lambda = V_{us}$ and $A\lambda^3(\rho - i\eta) = V_{ub}$.

resulting in an easy theoretical description at the parton level, even though uncertainties arise when introducing QCD calculations to describe the hadronization process. Given the fact that the b quark mass is considerably larger than the scale Λ_{QCD} that determines the low energy hadron physics, the total rate can be expanded in powers of Λ_{QCD}/m_b and α_S , separating perturbative and non-perturbative physics.

Two main experimental approaches are used to measure $|V_{ub}|$ from $\bar{B} \rightarrow X_u \ell \bar{\nu}$ decays, depending on the choice of integrating over all possible charmless final states or selecting a particular one: inclusive and exclusive. The first approach provides higher signal efficiency while the second gives a better background rejection. Theoretical inputs are needed by both approaches to model the hadronization but since they rely on independent calculations, they provide two complementary determinations of $|V_{ub}|$.

3. Experimental Techniques

The most recent measurements of charmless semileptonic B decays have been performed by *BABAR*, Belle and CLEO experiments. These experiments record e^+e^- collisions at the energy of $\Upsilon(4S)$, a $b\bar{b}$ bound state that decays predominantly in $B^0\bar{B}^0$ or B^+B^- mesons. The main backgrounds for $b \rightarrow u\ell\bar{\nu}$ transitions are the more abundant $b \rightarrow c\ell\bar{\nu}$ (~ 50 times larger), the continuum background coming from $e^+e^- \rightarrow q\bar{q}$, $q = (u, d, s, c)$ and, where applicable, combinatorial background due to random association of tracks in the reconstruction of a B meson. There are three established experimental techniques employed to select signal events, that differ on the reconstruction of the second B in the event (*tag* side), and are described below.

3.1. Untagged Method

In the untagged method the B recoiling against the signal B is not explicitly reconstructed. With this technique, the neutrino four-momentum is inferred from the difference between the momentum of the colliding beam particles and the sum of the momenta of all the charged and neutral particles detected in a single event. The kinematic consistency

of a B_{tag} candidate with a B meson decay is evaluated using two variables: the beam-energy substituted mass $m_{ES} \equiv \sqrt{s/4 - |p_B^*|^2}$, and the energy difference $\Delta E \equiv E_B^* - \sqrt{s}/2$. Here \sqrt{s} is the total CM energy, and p_B^* and E_B^* denote the momentum and energy of the B_{tag} candidate in the CM frame. For correctly identified B_{tag} decays, the m_{ES} distribution peaks at the B meson mass, while ΔE is consistent with zero.

The untagged method offers higher signal efficiency with respect to the other two methods but due to the poor resolution on the neutrino 4-momentum has lower purity.

3.2. Semileptonic Tag Method

In the semileptonic method, the $B \rightarrow D^{(*)}\ell\nu$ decay is reconstructed in the tag side. Several D and D^* decay modes are used for tagging. The presence of 2 neutrinos requires other kinematical constraints in order to separate signal events from backgrounds. With respect to the untagged method, the semileptonic tag provides lower efficiency but higher purity.

3.3. Hadronic Tag Method

In this method the tag side is reconstructed as a decay of the type $B \rightarrow D^{(*)}Y$, where Y represents a linear combination of charged and neutral pions and kaons. Several decay combinations are taken into account. ΔE and m_{ES} variables are used to check the consistency of the reconstructed B candidate. Since the B_{tag} is fully reconstructed, the kinematic of the event is completely constrained and charge and flavour of the signal B can be inferred. Given the good neutrino 4-momentum resolution provided by this method, other kinematical variables, such as the leptonic squared invariant mass q^2 , can be exploited to separate the background from the $b \rightarrow u$ signal events. The fallback of this method is the very low tag efficiency (at the order of 10^{-3}).

4. Exclusive $|V_{ub}|$ Determinations

In the exclusive approach, the measured branching fraction for a specific charmless decay channel, e.g. $B \rightarrow \pi\ell\nu$, is converted into $|V_{ub}|$ using theoretical calculations of the form factors (FF) which parametrize QCD effects. In particular, for $B \rightarrow \pi\ell\nu$ decays, the differential branching fraction as function of q^2 is proportional to $|V_{ub}||f_+(q^2)|$, the latter term of the product being the FF. Experiments measure $|V_{ub}||f_+(q^2)|$ and informations on the shape and normalization of $f_+(q^2)$ must come from theory. Several FF calculations are available, based on quark models [3], lattice QCD [4, 5] and Light Cone Sum Rules (LCSR) [6]. Lattice QCD and LCSR calculations have validity

on complementary q^2 ranges, giving predictions on $q^2 > 16 \text{ GeV}^2/c^4$ and $q^2 < 14 \text{ GeV}^2/c^4$ respectively.

With more and more statistics provided by the B -Factories, it has become possible to measure branching ratios on different q^2 intervals and compare the predicted FF shapes to experimental data. Figure 1 shows the differential partial branching ratio spectrum as function of q^2 for $B \rightarrow \pi\ell\nu$ decays measured with an untagged analysis performed by *BABAR* [7]. This analysis has shown that FF calculations based on quark models are not consistent with data distributions.

Table I lists a summary of branching ratio determinations for $B \rightarrow \pi\ell\nu$ decays. All the measurements are consistent inside the experimental uncertainties. Among all the methods, the untagged one provides the most precise measurement, having an uncertainty of approximately 7% in the branching ratio determination. The world average computed by the HFAG [11]

Table I $\mathcal{B}(B \rightarrow \pi\ell\nu)$ measurements for different experiments and tagging techniques. U, SL and Had indicate untagged, semileptonic tag and hadronic tag methods respectively. Errors on branching ratios are statistical and systematic.

| Mode | $B\bar{B}$ [10^6] | Branching Ratio [10^{-4}] | Exp./Tag |
|------------------------------------|--------------------------|----------------------------------|----------------------|
| $B^0 \rightarrow \pi^- \ell^+ \nu$ | 227 | $1.46 \pm 0.07 \pm 0.08$ | <i>BABAR</i> [7] U |
| | 15.4 | $1.37 \pm 0.15 \pm 0.11$ | CLEO [8] U |
| | 232 | $1.12 \pm 0.25 \pm 0.10$ | <i>BABAR</i> [9] SL |
| | 275 | $1.38 \pm 0.19 \pm 0.14$ | Belle [10] SL |
| | 232 | $1.07 \pm 0.27 \pm 0.15$ | <i>BABAR</i> [9] Had |
| $B^+ \rightarrow \pi^0 \ell^+ \nu$ | 232 | $0.73 \pm 0.18 \pm 0.08$ | <i>BABAR</i> [9] SL |
| | 275 | $0.77 \pm 0.14 \pm 0.08$ | Belle [10] SL |
| | 232 | $0.82 \pm 0.22 \pm 0.11$ | <i>BABAR</i> [9] Had |

group is $\mathcal{B}(B^0 \rightarrow \pi^- \ell^+ \nu) = (1.38 \pm 0.06 \pm 0.07) \times 10^{-4}$, where the first error is statistical and the second due to systematic uncertainties.

According to the various FF calculation, different $|V_{ub}|$ values can be computed and are shown in Fig. 2, for the full q^2 range. With the exclusive approach, the central value for $|V_{ub}|$ lies in the interval $[3.11, 3.80] \times 10^{-3}$, in good agreement with the indirect determination of $|V_{ub}|$ performed by UT fit collaboration: $|V_{ub}|_{UTfit} = (3.44 \pm 0.16) \times 10^{-3}$ [12]. The exclusive determinations are still limited by the theoretical uncertainties on the knowledge of the FF, that contribute up to 23% to the total error.

Branching ratio measurements of a B meson decaying into other charmless semileptonic final state (ρ , η/η' , ω) have been performed (world averages can be found on HFAG website [11]); however theory calculations necessary to convert these measurements into $|V_{ub}|$ values are not yet mature.

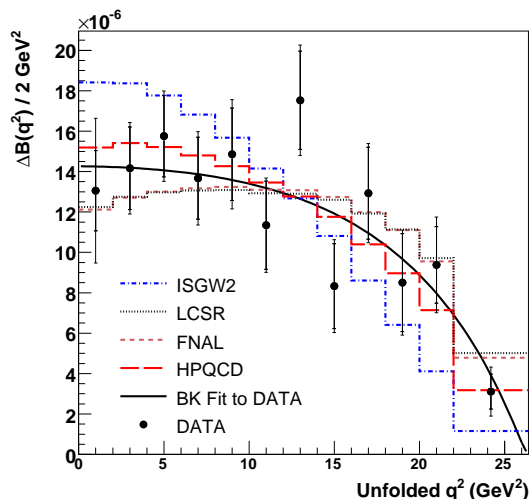


Figure 1: $\Delta\mathcal{B}(B \rightarrow \pi\ell\nu)$ as function of q^2 . The solid black curve shows the result of the fit of the BK parametrization [13] to the data. Other FF calculations [3–6] are also compared to data.

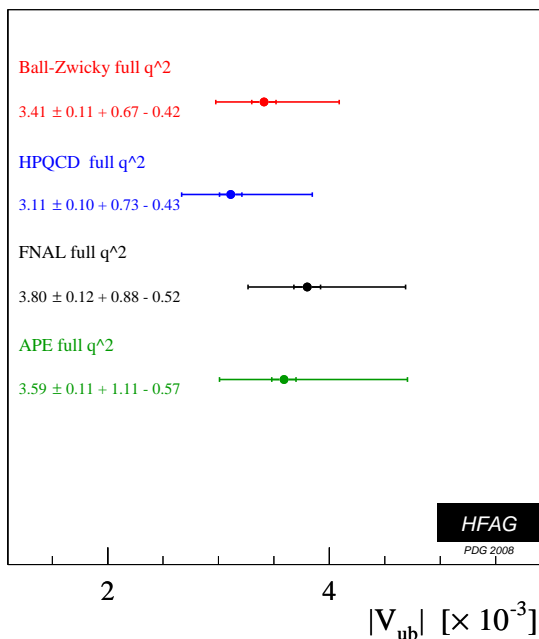


Figure 2: Comparison of exclusive $|V_{ub}|$ determinations for different form factor calculations for the full q^2 range.

5. Inclusive $|V_{ub}|$ Determinations

The full rate of inclusive charmless B decays is computed within the Operator Product Expansion (OPE) with a theory uncertainty of $\sim 5\%$, mainly due to uncertainty on the b quark mass. In practice the accessible rate is reduced since it is necessary to exploit kinematic variables that describe the semileptonic decays in order to suppress the overwhelming $b \rightarrow c$ transi-

tions; this restricts the measurement to phase space regions where particles containing charm cannot be produced. The drawback of this approach is on the theory side since calculating partial widths in regions of phase space where $\bar{B} \rightarrow X_c \ell \bar{\nu}$ are suppressed is very challenging, as the HQE convergence in these regions is spoiled and a non-perturbative distribution function, the shape function (SF)[14, 15], whose form is unknown, needs to be introduced. Weak annihilation and other non-perturbative effects need to be modeled too.

The shape function is a universal property of B meson at leading order, however sub-leading shape functions arise at each order in $1/m_b$ expansion. SF parameters can be constrained by measuring moments of inclusive distributions from $\bar{B} \rightarrow X_c \ell \bar{\nu}$ and $B \rightarrow X_s \gamma$ decays which are related to the same heavy quark parameters (m_b , the b quark mass and μ_π^2 , the kinetic energy of b quark in the B meson).

In the recent years, many theoretical calculations have become available, either based on OPE approach [16–19] or on models of non-perturbative QCD [20, 21].

Several kinematic variables are used to separate signal from $b \rightarrow c$ background, each having its own advantage. The lepton energy E_ℓ is the simplest to measure but the cut applied to reduce the charmed background restricts the total accessible signal rate to $\sim 10\%$; moreover the dependence on leading and subleading SF and weak annihilation corrections may be substantial. The squared leptonic invariant mass q^2 is weakly sensitive to SF effects, has higher accessible $b \rightarrow u$ fraction, $\sim 20\%$, but is sensitive to weak annihilation corrections. Much higher signal rate is provided by the hadronic invariant mass m_X and the light cone momentum $P_+ = E_X - |\vec{p}_X|$, $\sim 80\%$ and $\sim 70\%$ respectively, but both depend on SF and subleading SF corrections. The most recent inclusive $|V_{ub}|$ determinations have been performed by the BABAR experiment using the hadronic tag technique [22]. In this analysis, inclusive m_X , P_+ and (m_X, q^2) distributions have been reconstructed for semileptonic B decays and measurements of charmless partial branching fractions have been performed in regions of phase space where the $b \rightarrow c$ transitions are highly suppressed. Continuum and combinatoric backgrounds have been subtracted with fits to m_{ES} distributions. Figure 3 shows the fits of Monte Carlo $b \rightarrow c$ (blue), $b \rightarrow u$ (white) and other background (gray) shapes to the measured data (points) from which partial branching fractions for the signal enhanced region have been determined. $|V_{ub}|$ values have then been calculated using the relation

$$|V_{ub}| = \sqrt{\frac{\Delta\mathcal{B}(\bar{B} \rightarrow X_u \ell \bar{\nu})}{\tau_B \tilde{\Gamma}_{thy}}} \quad (1)$$

where τ_B is the B lifetime and $\tilde{\Gamma}_{thy}$ are the the-

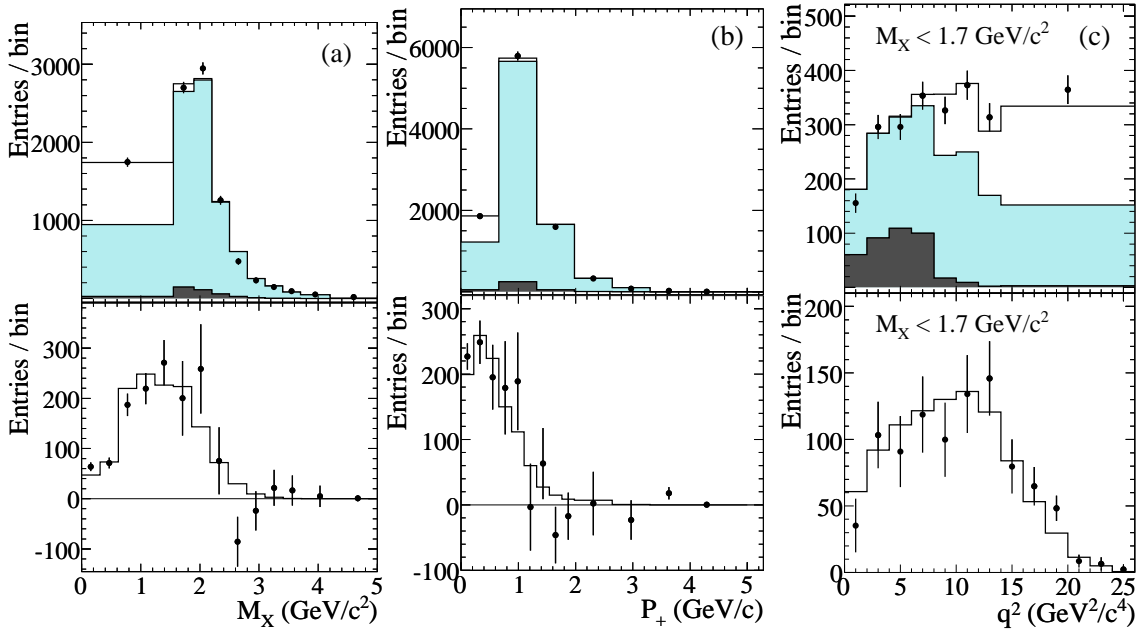


Figure 3: Upper row: Measured m_X (a), P_+ (b) and q^2 with $m_X < 1.7 \text{ GeV}/c^2$ (c) spectra (data points). The result of the fit to the sum of three Monte Carlo contributions is shown in the histograms: $\bar{B} \rightarrow X_u \ell \bar{\nu}$ decays generated inside (white) and outside (gray) the signal region, and $\bar{B} \rightarrow X_c \ell \bar{\nu}$ and other background (blue). Lower row: corresponding spectra for $\bar{B} \rightarrow X_u \ell \bar{\nu}$ after $\bar{B} \rightarrow X_c \ell \bar{\nu}$ and other background subtraction, rebinned to show the shape of the kinematical variables.

oretical acceptances provided by the cited models. The $|V_{ub}|$ determinations obtained are in good agreement with the ones provided in a similar analysis by Belle [23], and show that the measurements based on m_X and (m_X, q^2) are compatible with theory calculations, while there is a hint that results based on P_+ are somewhat lower than theory predictions and closer to $|V_{ub}|$ determinations which use exclusive charmless semileptonic decays.

HFAG provides world averages of $|V_{ub}|$ values obtained within the currently available theoretical frameworks and are listed in Fig. 4. Inclusive charmless semileptonic decays give $|V_{ub}|$ determinations that are compatible with exclusive ones, even though with higher values. Similarly for the exclusive measurements, the dominant uncertainty is due to theory ($\sim 7\%$).

6. Weak Annihilation

Weak annihilation denotes a $B^+ \rightarrow X_u \ell^+ \nu$ decay in which the \bar{b} and the spectator u quark forming the B^+ meson annihilate into a W^+ boson, and a hard gluon emitted in the interaction materializes into a charmless final state. The contribution to the total charmless semileptonic rate is expected to be small, of the order of 3%, but can be relevant when selecting large q^2 regions. Weak annihilation can be experimentally observed as a difference in the partial decay rates

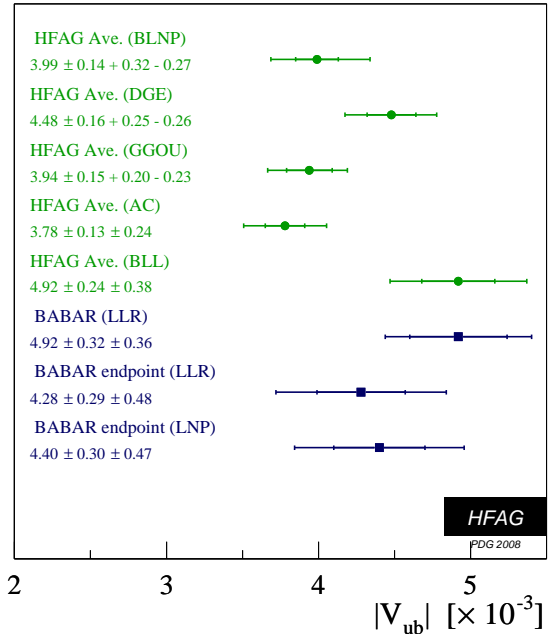


Figure 4: Comparison of inclusive $|V_{ub}|$ values obtained using different theoretical calculations.

of $B^0 \rightarrow X_u^- \ell^+ \nu$ and $B^+ \rightarrow X_u^0 \ell^+ \nu$ at high q^2 since it occurs only for charged B meson. Measurements performed by *BABAR* [24] and *CLEO* [25] have provided no evidence of weak annihilation so far, placing the

upper limit: $\Gamma_{WA}/\Gamma_{b\rightarrow ul\nu} < 8\%$ at 90% CL.

7. Conclusion

The large datasets collected at the B -Factories, and the increased precision of theoretical calculations, allowed an improvement in the determination of $|V_{ub}|$. However, there are still significant uncertainties. In the exclusive approach, the most precise measurement of the pion channel branching ratio is obtained by untagged analysis. This very good precision can be reached by tagged analysis with more data. The problem with exclusive decays is that the strong hadron dynamics can not be calculated from first principles and the determination of the form factor has to rely on light-cone sum rules or lattice QCD calculations. The current data samples allow to compare different FF models with data distributions. With further developments on lattice calculations, the theoretical error should shrink to reach the experimental one.

The inclusive approach still provides the most precise $|V_{ub}|$ determinations. With new theoretical calculations, the mild (2.5σ) discrepancy with respect to the $|V_{ub}|$ value determined from the global UT fit has been reduced. Anyway, as in the exclusive approach, theory uncertainties represents the limiting factor to the precision of the measurement. Reducing the theoretical uncertainties to a level comparable with the statistical error is challenging. New measurements in semileptonic decays of charm mesons could increase the confidence in theoretical calculations and related uncertainties.

References

- 1 M. Kobayashi and T. Maskawa, Prog. Theor. Phys. **49**, 652 (1973).
- 2 O. Buchmüller and H. Flächer, Phys. Rev. **D73**, 073008 (2006).
- 3 D. Scora and N. Isgur, Phys. Rev. D **52**, 2783 (1995).
- 4 HPQCD Collaboration, E. Gulez *et al.*, hep-lat/0601201.
- 5 FNAL Collaboration, M. Okamoto *et al.*, hep-lat/0409116.
- 6 P. Ball and R. Zwicky, Phys. Rev. D **71**, 014015 (2005).
- 7 BABAR Collaboration, B. Aubert *et al.*, Phys. Rev. Lett. **98**, 091801 (2007).
- 8 CLEO Collaboration, N. E. Adam *et al.*, Phys. Rev. Lett. **99**, 041802 (2007).
- 9 BABAR Collaboration, B. Aubert *et al.*, Phys. Rev. Lett. **97** 211801 (2006).
- 10 Belle Collaboration, T. Hokuue *et al.*, Phys. Lett. **B648**:139-148 (2007).
- 11 Heavy Flavour Averaging Group (HFAG), <http://www.slac.stanford.edu/xorg/hfag>
- 12 <http://www.utfit.org>
- 13 D. Becirevic and A. B. Kaidalov, Phys. Lett. **B478**, 417 (2000).
- 14 M. Neubert, Phys. Rev. **D49**, 4623 (1994); *ibid.* **D49**, 3392 (1994).
- 15 I. Bigi *et al.*, Int. J. Mod. Phys. **A9**, 2467 (1994).
- 16 B. O. Lange *et al.*, Phys. Rev. D **72**, 073006 (2005).
- 17 B. O. Lange *et al.*, JHEP 0510, 084, (2005).
- 18 C. W. Bauer *et al.*, Phys. Rev. **D64**, 113004 (2001).
- 19 P. Gambino *et al.*, JHEP 10, 058 (2007).
- 20 J. R. Andersen and E. Gardi, JHEP 0601, 097 (2006).
- 21 U. Aglietti *et al.*, Phys. Rev. **D74**, 034004 (2006); *ibid.*, **D74**, 034005 (2006), *ibid.* **D74**, 034006 (2006).
- 22 BABAR Collaboration, B. Aubert *et al.*, Phys. Rev. Lett. **100**, 171802 (2008).
- 23 Belle Collaboration, I. Bizjak *et al.*, Phys. Rev. Lett. **95**, 241801 (2005).
- 24 BABAR Collaboration, B. Aubert *et al.* arXiv:0708.1753 [hep-ex].
- 25 J. L. Rosner *et al.*, CLEO Collaboration, Phys. Rev. Lett. **96**, 121801 (2006).